FIRE AND MATERIALS
Fire Mater. 2009; **33**:223–243
Published online 20 April 2009 in Wiley InterScience (www.interscience.wiley.com). DOI: 10.1002/fam.999

Fire performance of bolted connections in laminated veneer lumber

P. J. Moss[1,*,†], A. H. Buchanan[1], M. Fragiacomo[2], P. H. Lau[3] and T. Chuo[4]

[1]*Department of Civil Engineering, University of Canterbury, Private Bag 4800, Christchurch 8140, New Zealand*
[2]*Department of Architecture and Planning, University of Sassari, Alghero, Italy*
[3]*Arup Fire, Perth, WA, Australia*
[4]*Beca Fire International, Wellington, New Zealand*

SUMMARY

This paper describes an investigation into the fire performance of bolted tensile connections in laminated veneer lumber (LVL) made from radiata pine. The capacity of the bolted connections depends on the embedment strength of the wood and on the yield moment of the bolts. The purpose of the research was to develop a prediction method for the time to failure of the connections when exposed to fire. An experimental investigation was carried out on the axial tensile strength of three types of bolted connections that utilized either wood or steel splice plates. Some specimens were tested at ambient temperatures while similar specimens were tested in fire conditions with a constant applied load. In addition, single-bolted connections were tested under constant elevated temperature conditions to determine the embedment strength of the LVL. Connections with no steel plates, or with steel plates slotted between the timber members, performed better than those with exposed steel. A simplified design approach is proposed, using an extension of the Johansen formulae, such that the embedment strength of the LVL depends on the temperature in the bolt. Copyright © 2009 John Wiley & Sons, Ltd.

Received 3 February 2009; Revised 17 February 2009; Accepted 17 February 2009

KEY WORDS: timber; bolted connection; fire tests; laminated veneer lumber; embedment strength; charring rate

1. INTRODUCTION

Fire is unpredictable and dangerous, especially in residential buildings. The effect of fire on timber structural members is very complex because of the large number of variables involved. Once ignition has occurred, then a layer of char forms as the wood burns. A structural wood member will

*Correspondence to: P. J. Moss, Department of Civil Engineering, University of Canterbury, Private Bag 4800, Christchurch 8140, New Zealand.
†E-mail: peter.moss@canterbury.ac.nz

Contract/grant sponsor: Carter Holt Harvey

lose load capacity as the wood is converted to charcoal, which has no strength. The thickening char layer protects the remaining wood, resulting in a predictable rate of charring below the surface. The rate of development of this charred layer determines how long the member can continue to carry load before the strength of the remaining unburned wood is exceeded. A thin layer of heat-affected wood below the char layer will have reduced strength and stiffness.

In recent years, a number of research papers have been published on the influence of temperature on the mechanical properties of wood (e.g. [1–4]). Research has also been carried out into the performance of joints in timber members when subjected to fire temperatures (e.g. [5–9]). Particular research into the embedment strength of wood at elevated temperatures has also been carried out by Moraes *et al.* [10] and Chapuis *et al.* [11]. They carried out embedment tests at temperatures ranging from 20 to 240°C. These specimens of timber plus 8 mm diameter dowels were heated for 110 min in an oven, then placed in a temperature-controlled chamber on the test machine and kept at the test temperature for a further 10 min before testing to a maximum displacement of 5 mm.

This paper describes an experimental investigation carried out to determine the axial tensile strength of fire-exposed laminated veneer lumber (LVL) members with three types of bolted connections utilizing either wood or steel splice plates. The arrangements tested were wood–wood–wood (W–W–W), steel–wood–steel (S–W–S) and wood–steel–wood (W–S–W). Some specimens were tested at ambient temperatures to determine the ultimate strength, while similar specimens were tested in fire conditions under constant applied load. The purpose of the research was to develop a prediction method for the time to failure of the connections when exposed to fire. In addition, single-bolted connections were tested under constant temperature conditions to determine the embedment strength of the LVL [12] over a range of temperatures. The variation in the embedment strength was then used in Johansen's equations (as presented in EC5 [13]) to predict the failure of single-bolted connections between LVL members [12] as well as multi-bolted connections [12, 14]. The full test series included bolts, dowels, nails, screws and proprietary connectors but this paper reports only bolted joints, with the tests on others reported elsewhere [14].

2. TESTS CARRIED OUT

Testing was carried out on three arrangements as shown in Figure 1 for both single- and multi-bolted connections. The design of the multi-bolted connection was based on a tensile member in the bottom chord of a floor or a roof truss. The timber (LVL) members being joined were 150×63 mm. The LVL side plates were 150×45 mm. The design properties of the LVL are shown in Table I [15]. The steel plates (side or central) were 6 mm thick. All bolts were 12 mm in diameter and were made of Grade 4.6 steel.

The design load on the joint was taken to be 40% of the ultimate tensile strength of the LVL in cold conditions (i.e. a load of 40% of 221 kN = 88 kN) by assuming that other design conditions will be more critical than the tensile strength of the member. With a calculated load factor of 0.33 for fire conditions, this gave an expected fire load of 29 kN. Six bolts were used for the W–W–W joint, four bolts for the S–W–S joint and five bolts for the W–S–W joint. The different connections were fabricated as shown in Figures 2–4.

The same size timber and steel members and bolts were used to fabricate single-bolt joints. The bolts were placed on the member centreline with an end distance of 100 mm.

DOI: 10.1002/fam

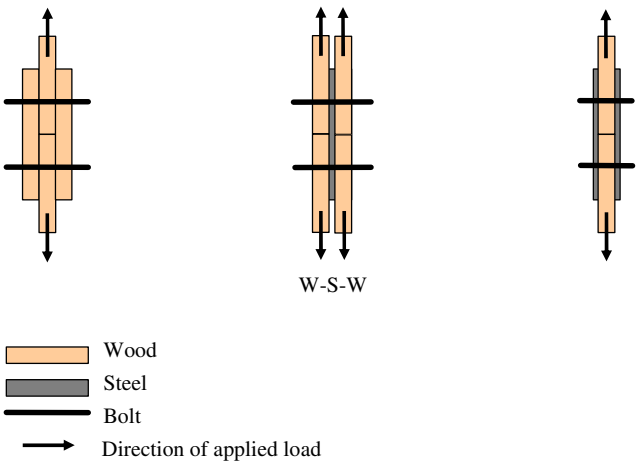

Figure 1. Joint arrangements as tested.

Table I. Limit state properties for design with Hyspan [15].

Elastic moduli		
Modulus of elasticity (MPa)	E	13 200
Modulus of rigidity (MPa)	G	660
Characteristic strength		
Bending (MPa)	f'_b	42
Tension parallel to grain (MPa)	f'_t	27
Compression parallel to grain (MPa)	f'_c	34
Shear in beams (MPa)	f'_s	4.5
Compression perpendicular to grain (MPa)	f'_p	12

3. COLD TESTING

All the joints were tested at ambient temperatures to ascertain the likely ultimate strength relative to the design load. This testing was carried out in compression, rather than tension. The deflection was measured as the load was applied, with one potentiometer on each side. Typical results are illustrated in Figure 5 and show only a small variation between tests. Failure was caused by longitudinal splitting in the LVL at the bolt positions. A greater end distance could be used to increase the failure load; however, this is considered unnecessary as the failure loads in all the tests were already 100–150% higher than the design load in the New Zealand timber design code [16].

4. FIRE TESTING

A custom-built testing frame and furnace allowed each specimen to be held under constant load while exposed to simulated fire conditions (Figure 6). Each test specimen was positioned and the air supply was regulated so that the heated specimen was subjected to approximately uniform

DOI: 10.1002/fam

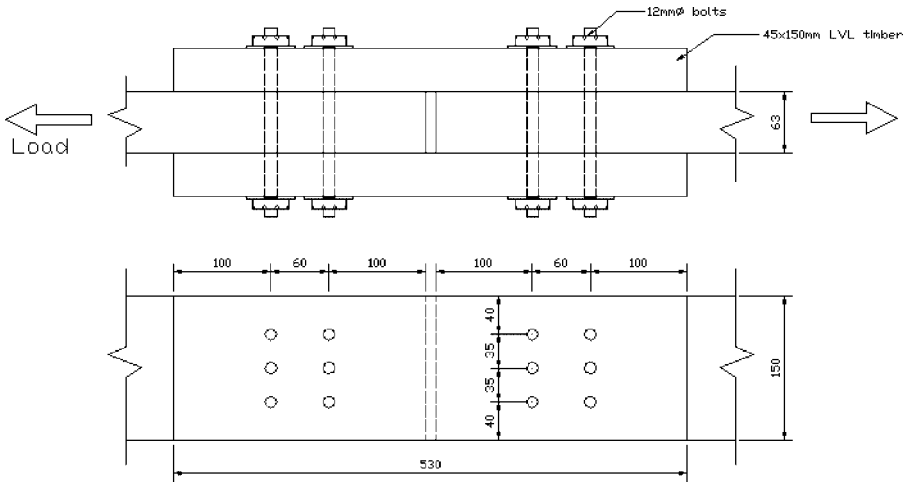

Figure 2. Arrangement of bolted connections for W–W–W tests (dimensions in mm).

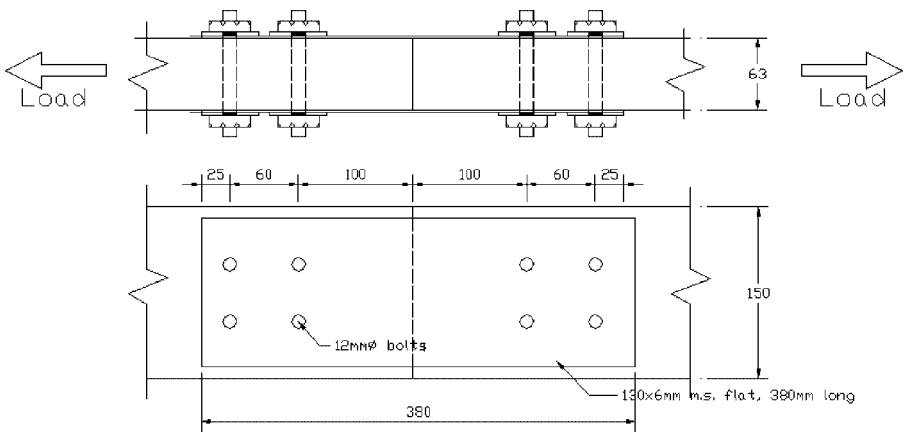

Figure 3. Arrangement of bolted connections for S–W–S tests (dimensions in mm).

charring on all sides. Figure 7 shows that the heating from the electric coils in the furnace was not able to heat the furnace as rapidly as the standard ISO 834 fire curve [17] and the two curves for the furnace tests with the specimens in place were typical of the variations that occurred between tests.

Each specimen took between 2 and 5 min to begin charring, as evidenced by smoke coming from the furnace. The surfaces of the test specimens were not visible from outside the furnace. This led to a period where the test specimens were charring and building up gaseous pyrolysis products within the furnace, but prior to flaming [18]. After a few more minutes, the gases reached their unpiloted ignition temperature and ignited. There were flames on all surfaces of the test specimens from the time of ignition until the conclusion of the test.

DOI: 10.1002/fam

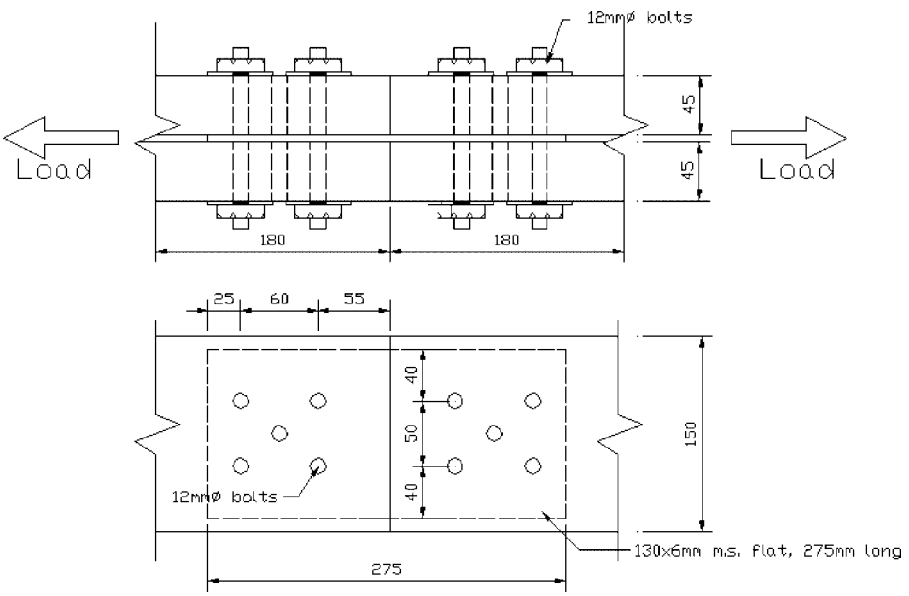

Figure 4. Arrangement of bolted connections for W–S–W tests (dimensions in mm).

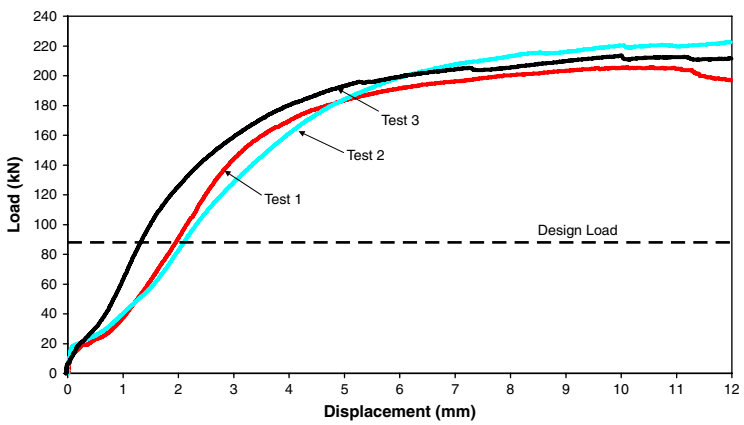

Figure 5. Strength of three W–S–W bolted joints at ambient temperatures.

When each test specimen had failed, the furnace was switched off and the specimen was quickly removed from the furnace. The flames were then extinguished and the specimen cooled with water to prevent further charring.

4.1. Time to failure

Each specimen was loaded with a constant load of 29 kN before starting the fire test. Time measurement started when the furnace was turned on. The failure time was the time at which the

DOI: 10.1002/fam

Figure 6. The test frame and furnace used for fire testing.

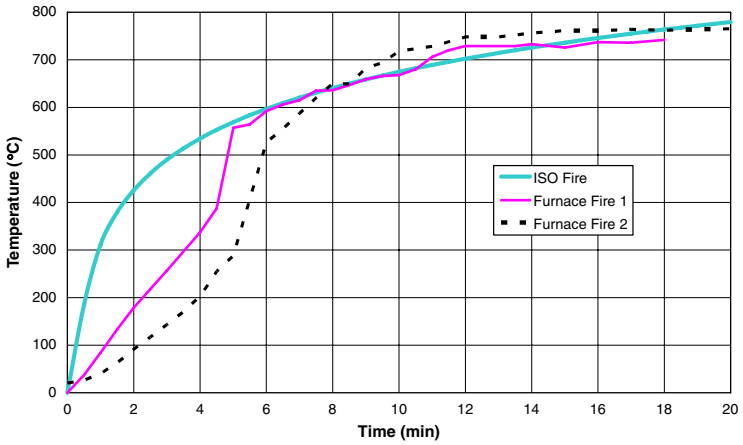

Figure 7. Comparison between ISO 834 fire curve and furnace temperatures for two typical tests.

load was not able to be sustained. The results are given in Table II. Figures 8–10 show typical connections after testing. Not only has the LVL suffered considerable charring, but the bolts have cut elongated slots in the LVL as they heated up during the fire.

4.2. Prediction of fire resistance

Because the furnace did not follow the standard ISO 834 fire, the time of failure in the tests was not the same as the fire resistance of the connections. To convert from the time of failure to an

DOI: 10.1002/fam

Table II. Average time to failure for bolted connections in fire testing.

Connections	Time to charring (min)	Time to ignition (min)	Time to failure (min)
W–W–W	2.9	4.5	22.5
S–W–S	3.3	4.5	11.4
W–S–W	3.1	4.3	19.3

Figure 8. Failure mode of W–W–W bolted connection after fire tests.

estimated fire resistance, the fire severity on the surface of the timber piece and the rate of char were analysed.

During a fire, a layer of char forms over the surface of unburnt timber, which then shrinks and burns away after a period of time. The fire resistance of a timber member with no connection is related to the residual cross section after charring. The base of the char layer is at approximately 300°C, with a heated layer below the char front. The part of this layer above 200°C is known as the pyrolysis zone, which is undergoing thermal decomposition into gaseous pyrolysis products, accompanied by loss of weight, loss of strength and discolouration [19].

To assess the charring rate of the timber, the char layer was removed after testing and the remaining timber section was measured. The depth of char and rate of char in Table III are averages over the duration of the test, which is the observed depth of char divided by the total duration of exposure, including the period at the beginning of the test before the onset of char. This was consistent with the testing procedure of Lane *et al.* [20] who provided the standard ISO 834 charring data used for comparison by Harris [18] and for the testing reported herein.

The charring rates for the test specimens in the furnace range from 0.53 mm/min up to 0.70 mm/min, with a mean value of 0.65 mm/min. This was slightly lower than the average charring rate observed in the ISO 834 furnace by Lane *et al.* [20] of 0.72 mm/min. Harris [18]

DOI: 10.1002/fam

Figure 9. Failure mode of S–W–S bolted connection after fire tests.

Figure 10. Failure mode of W–S–W bolted connection after fire tests.

developed a formula to convert the failure time in the furnace to failure time in a standard fire (fire resistance):

$$t_{\mathrm{ISO}} = \frac{c_{\mathrm{cust}}}{c_{\mathrm{ISO}}} t_{\mathrm{cust}} \tag{1}$$

where t_{ISO} is the fire resistance time in ISO furnace (min), t_{cust} is the time to failure in the custom furnace (min), c_{ISO} is the char rate recorded in the ISO furnace (0.72 mm/min) and c_{cust} is the char rate recorded in the custom furnace (mm/min).

DOI: 10.1002/fam

Table III. Calculated fire resistance using the charring rate method.

Connections	Time to failure (min)	Depth of char (mm)	Average char rate (mm/min)	Calculated fire resistance (min)	Fire resistance from fire severity correlation (min)	Difference in fire resistance (min)
W–W–W	22.5	15	0.67	21.2	20.5	0.7
S–W–S	11.4	6.5	0.57	9.2	8.8	0.4
W–S–W	19.3	11.5	0.60	16.3	16.5	−0.2
	Mean char rate (mm/min)		0.65			

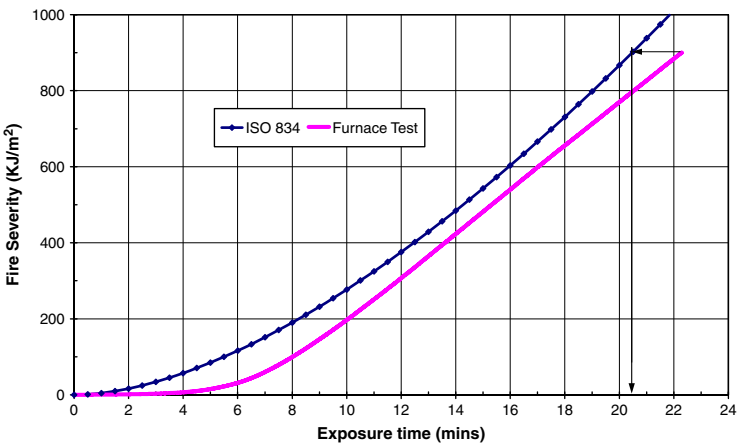

Figure 11. Correlation between time of exposure and fire severity for W–W–W bolted connection. The upper curve shows ISO fire severity and the lower curve shows the custom furnace exposure.

The actual durations in the furnace were converted to expected durations in the ISO fire, or the fire resistance, using Equation (1). The results are given in Table III.

The fire resistance of the connections was also determined using the 'total radiant heat exposure' concept suggested by Nyman [21]. In this method, the measure of fire severity is the cumulative radiant heat exposure at any time. The radiant heat exposure in the test fire can be compared with that in the ISO 834 fire to give an equivalent fire resistance. For example, in Figure 11 the fire severity curve for the connection is similar in shape to the fire severity curve of the ISO 834 fire curve, and the test connection failed at 22.5 min, which is equivalent to 20.5 min exposure to the standard fire. This method of comparing the severity of two different fires is considered to be more accurate than the traditional method of using the areas under the time–temperature curves [21].

The comparison between the fire resistance found using the mean charring rate and the fire severity correlation is also given in Table III. There is only a slight difference in fire resistance of the connections found from the charring rate and that found using the fire severity correlation.

DOI: 10.1002/fam

König [22] states that for connections with side members of wood, i.e. the W–W–W and W–S–W connections, fire resistance duration of 15 min for bolted connections is achievable. This can be seen to be in line with this research where the fire resistance of a W–W–W joint was estimated to be 21.2 min and that of a W–S–W joint to be 16.3 min.

5. HEATED TESTING

In order to develop a simple method of predicting the load capacity and deformation of connections in timber structures when exposed to known heat flux, a series of tests were carried out at known temperatures in a similar manner to that outlined in previous research [10, 11]. For this testing, a series of single-bolt joints were heated in the furnace for 2 h at a constant temperature with no applied load under temperatures ranging from ambient to 250°C, and then quickly loaded to failure.

5.1. Embedment strength versus temperature

Since the S–W–S connections were similar to standard embedment specimens, the results from these tests were used to estimate the embedment strength for the LVL at elevated temperatures. The main differences between the single-bolt joints tested and the testing apparatus as required by ISO 10984-2 [23] are outlined in Table IV.

In the ISO standard, the 'embedding strength' is based on either the maximum load or the load carried at 5 mm displacement, depending on which occurs first. As the bolted connection tested contained two bolts (one at each member end as shown in Figure 12) and the maximum load occurred at a large displacement, the embedment strength was calculated by dividing the load at 10 mm displacement by the bolt diameter and the thickness of the member. Figures 13–15 show the load–displacement relationships for S–W–S, W–S–W and W–W–W connections after correcting for initial slip. The joint strengths at different temperatures were then substituted into the relevant Johansen yield formulae as given in EC5 [13] to determine the embedment strengths. Other information required included the bending strength of the bolt at the various temperatures, the timber thickness and the experimental failure mode. The results for the calculated embedment strength are shown in Figure 16 where it can be seen that the embedment strength decreases as the temperature increases, reaching a minimum at about 120°C, and then increasing as the temperature increases further to 200°C. The reason for this increase is not clear and it is suggested that for design purposes the embedment strength should conservatively be taken as the lower value given by the dashed line until the reliability and extent of this increase in embedment strength can be assured by further testing. Figure 16 also shows the embedment strength determined using 45 mm thick LVL

Table IV. Comparison of single-bolt connection and ISO standard embedment test [23].

	Single-bolted S–W–S connection	ISO standard embedment test
1.	Steel members tightly bolted to timber member (Figure 12)	No contact between steel members and test specimen
2.	Two fasteners were used in each test (i.e. one at each member end)	Only one fastener used in test

DOI: 10.1002/fam

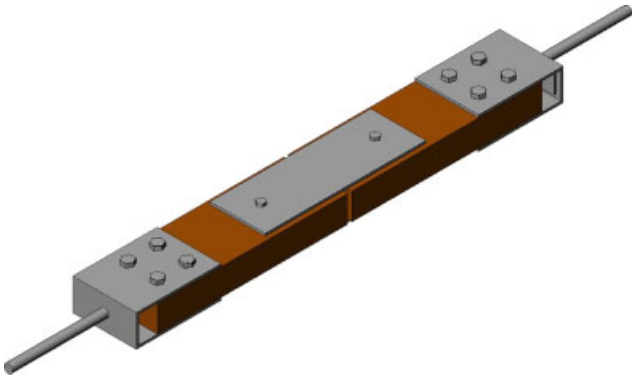

Figure 12. The single-bolt S–W–S connection used for the heated and fire tests.

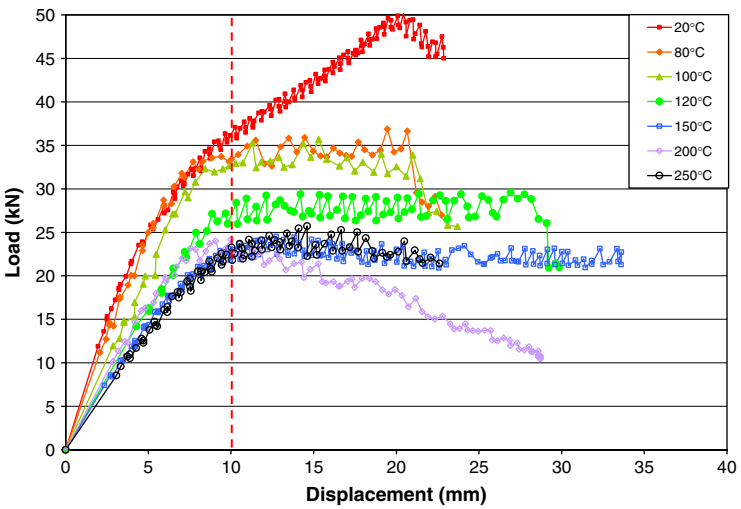

Figure 13. Load–displacement curves for single-bolted joints in a S–W–S connection at various temperatures.

and 12 mm thick splice plates, where the thinner thickness of LVL fully complies with the thickness to bolt diameter ratio recommended by the ISO standard [23] for embedment strength tests.

5.2. Prediction of failure load versus temperature

The temperatures of the air, steel plates and at several points on the bolts were measured using thermocouples and are shown in Figure 17 for the S–W–S connection during the fire test. It can be seen that the temperatures of the steel side plates and the bolts are effectively the same.

Figure 18 shows the temperature of the air, steel plates and at several points on the bolts for the W–S–W connections during the fire test. It can be seen that the temperatures of the bolt head and at the middle of the side members were similar (leaving aside the discrepancy in one thermocouple),

DOI: 10.1002/fam

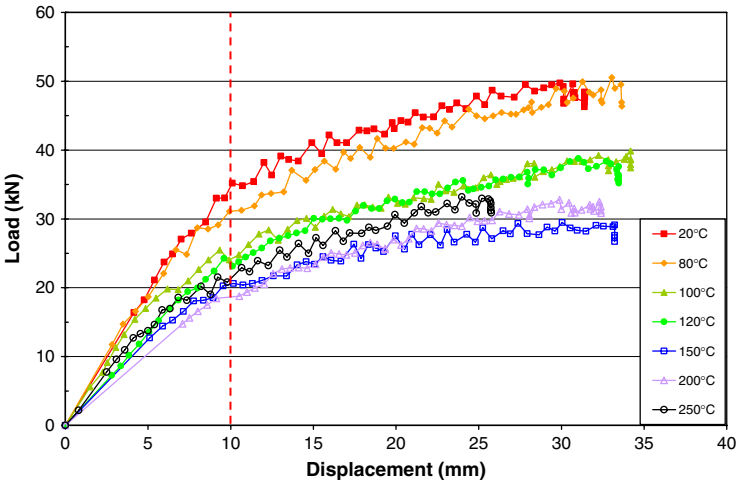

Figure 14. Load–displacement curves for single-bolted joints in a W–S–W connection at various temperatures.

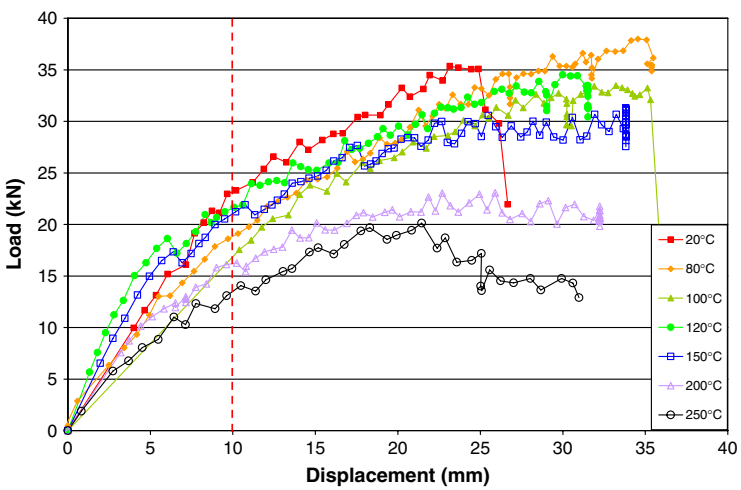

Figure 15. Load–displacement curves for single-bolted joints in a W–W–W connection at various temperatures.

while the temperature in the bolt at the steel plate is considerably lower but similar to those in the timber members. In the case of the W–W–W connections, Figure 19 shows that the temperature varies considerably throughout the joint.

Using the embedment strength determined in Section 5.1, the failure loads predicted by each of the European yield formulae [13] at each temperature were calculated for the single-bolt S–W–S, W–S–W and W–W–W connections and are shown in Figures 20–22, together with the experimental

DOI: 10.1002/fam

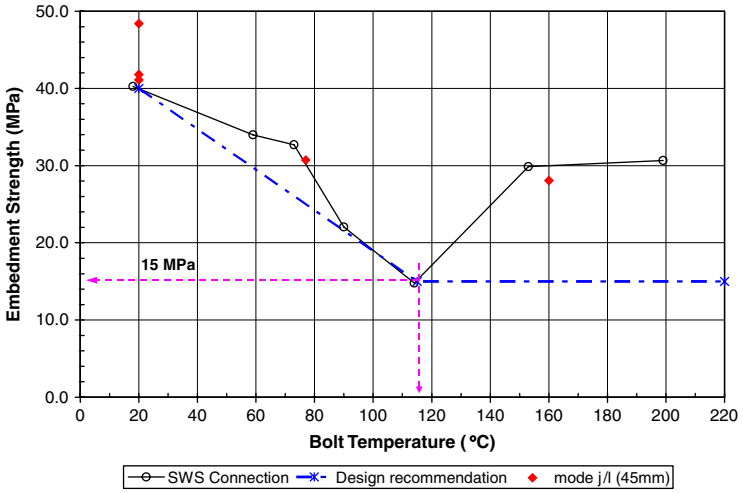

Figure 16. Experimental and modified embedment strength for LVL.

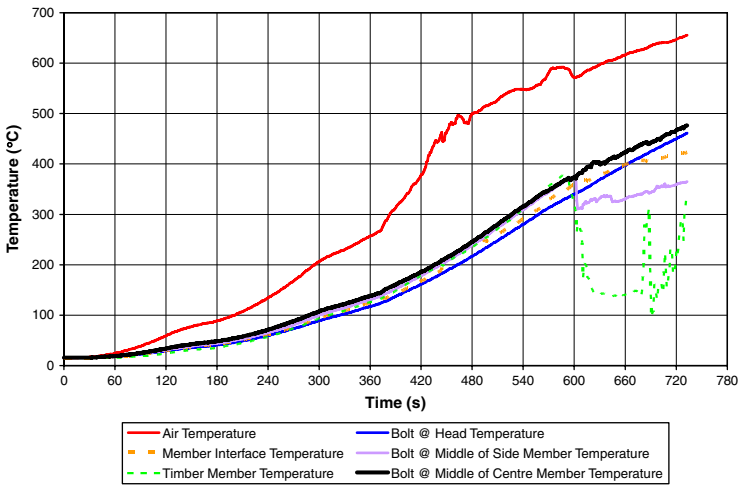

Figure 17. Temperatures measured within the S–W–S connection during the fire test.

failure loads for each relevant failure mode. All the possible failure modes for each connection type are shown in Table V, along with the relevant Johansen yield equation.

For the S–W–S connections, the experimental failure mode for the bolt temperatures up to 120°C was mode k whereas for temperatures above 150°C the failure mode was mode j/l. Figure 20 shows the predicted failure loads for mode j/l to be conservative for temperatures up to 120°C as they predict lower failure loads than were observed. For temperatures above 150°C, the predictions for failure in modes k and m are higher than found experimentally.

DOI: 10.1002/fam

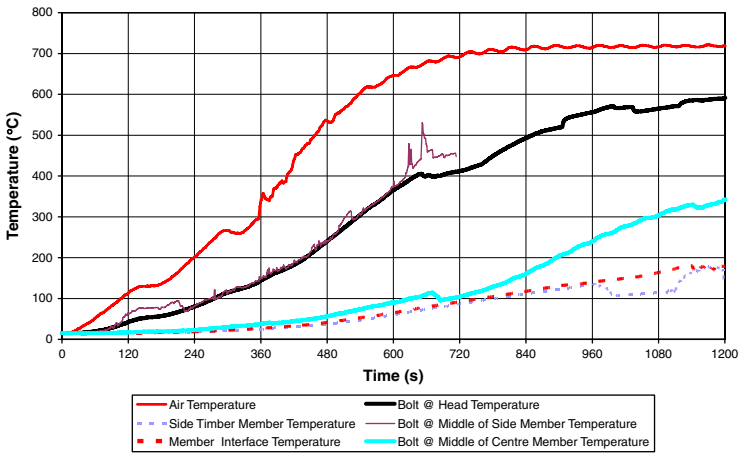

Figure 18. Temperatures measured within the W–S–W connection during the fire test. The results for the bolt temperature at the middle of the side member were terminated at the point where the thermocouple failed.

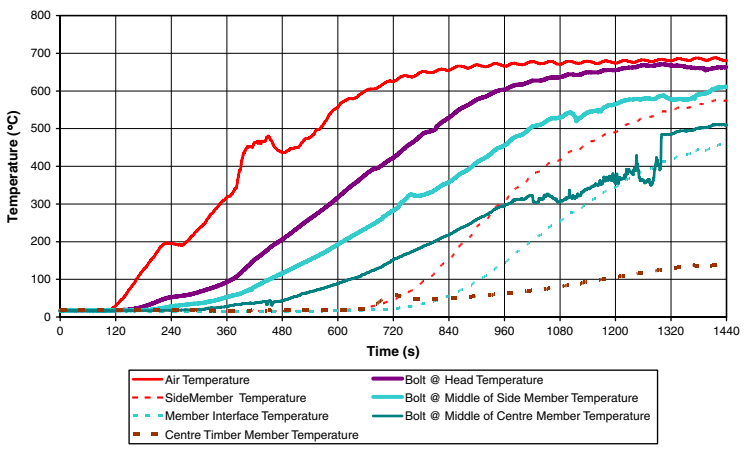

Figure 19. Temperatures measured within the W–W–W connection during the fire test.

For W–S–W connections, the predictions in Figure 21 based on the embedment strengths of Figure 16 show that up to a bolt temperature of 80°C failure mode *g* is the most probable failure mode. The experimentally observed failure mode generally agreed with the predicted failure mode. Above 90°C the predicted failure mode is failure mode *f* though the experimental results are a closer match to failure mode *g*.

The prediction of the W–W–W connections using Johansen's equations in Figure 22 shows that failure mode *h* is the most probable failure. The experimentally observed failure mode showed that failure mode *h* occurred over the range from 20 to 140°C. This agreed with the predicted failure mode though the match was more variable than that for the S–W–S and W–S–W connections.

DOI: 10.1002/fam

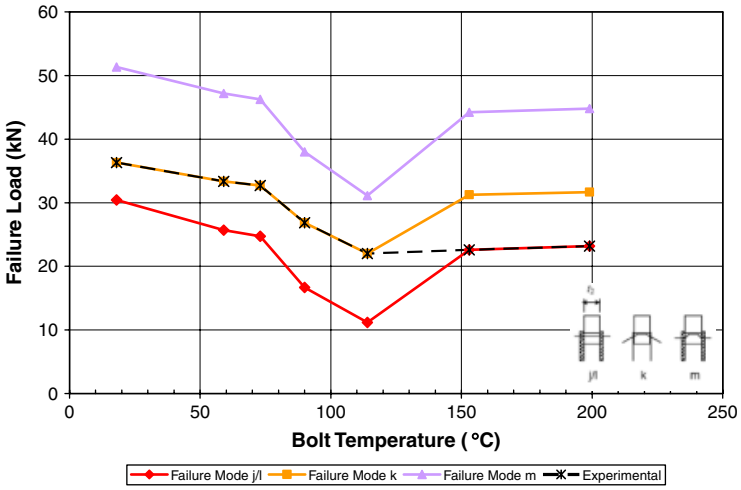

Figure 20. Predicted and experimental failure loads for single-bolt S–W–S connections tested at a constant temperature.

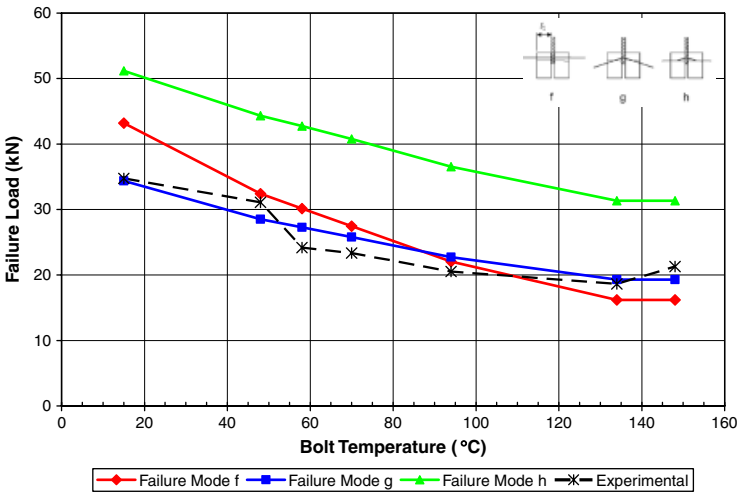

Figure 21. Predicted and experimental failure loads for single-bolt W–S–W connections tested at a constant temperature.

6. PREDICTION OF LOAD CAPACITY VERSUS TIME

Using the experimental embedment strength calculated above, the predicted failure loads in simulated fire tests for the three types of connections tested by Lau [14] (Figures 2–4) are shown in Figures 23–25.

DOI: 10.1002/fam

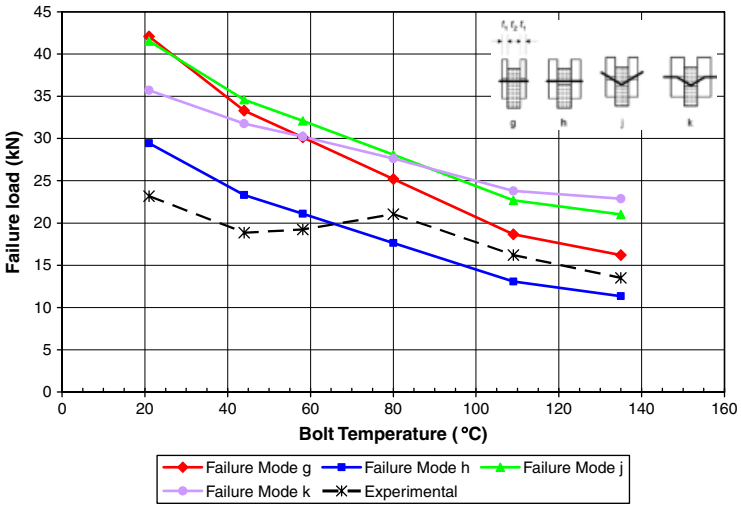

Figure 22. Predicted and experimental failure loads for single-bolt W–W–W connections tested at a constant temperature.

Initially, the contact thickness between the bolt and the timber members was taken as the original thickness less the thickness of the charred surface as indicated in Figure 26(a), given by

$$t_{\text{contact}} = t - (n \times D \times \theta) \tag{2}$$

where t is the original timber thickness (mm), n is the number of charring surfaces (–) ($n = 2$ for S–W–S, otherwise $n = 1$), D is the experimental charring rate (mm/min) and θ is the charring duration (min).

The failure loads predicted by the failure formulae were compared with the experimental failure results from fire tests carried out by Chuo [12] on both single-bolt and multi-bolt connections. These comparisons showed some large discrepancies and as a result a modified model was proposed wherein a char rounding effect at the edges of the bolt holes was included. This effect was observed in the test specimens at the end of the fire test and is illustrated in Figure 26(b) with the bolt to timber contact length being given by

$$t_{\text{contact}} = t - (2n \times D \times \theta) \tag{3}$$

where the quantities have the same meaning as those for Equation (2), and the factor 2 accounts for the char rounding effect at the edges of the bolt hole.

The predicted failure loads using the temperature-dependent embedment strength and Equation (3) for the three types of connection as tested by Lau [14] are shown in Figures 23–25 with several different failure modes for each prediction. Such figures show that the prediction of the failure mode and the failure load using the bi-linear embedment strength curve, together with the experimental charring rate and steel strength reduction factor for temperature, was reasonably accurate. However, the estimation of the failure time was less accurate, particularly for the S–W–S connection. This is because after the LVL had reached its constant embedment strength at 120°C (Figure 16), the load carrying capacity of the connection reduces only slightly as the timber chars. Therefore, the predicted failure time is very sensitive to the predicted load level.

DOI: 10.1002/fam

Table V. Johansen's yield equations [13] for resistance per shear plane per fastener* and (A) list of variables used in Johansen's equations.

Connection	Failure mode		Equation
S–W–S	*k*	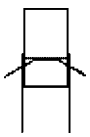	$F_{v,Rk}=1.25\{1.15\sqrt{2M_{y,Rk}f_{h,2,k}d}\}$
	j or *l*	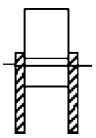	$F_{v,Rk}=0.5f_{h,2,k}t_2d$
	m	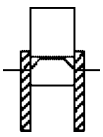	$F_{v,Rk}=1.25\{2.3\sqrt{M_{y,Rk}f_{h,2,k}d}\}$
W–S–W	*f*	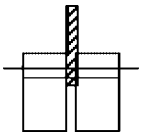	$F_{v,Rk}=f_{h,1,k}t_1d$
	g	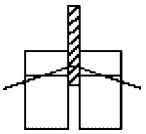	$F_{v,Rk}=1.25\left\{f_{h,1,k}t_1d\left[\sqrt{2+\frac{4M_{y,Rk}}{f_{h,1,k}dt_1^2}}-1\right]\right\}$
	h	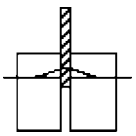	$F_{v,Rk}=1.25\{2.3\sqrt{M_{y,Rk}f_{h,1,k}d}\}$
W–W–W	*g*	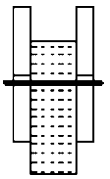	$F_{v,Rk}=f_{h,1,k}t_1d$
	h	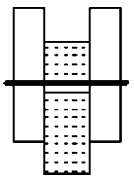	$F_{v,Rk}=0.5f_{h,2,k}t_2d$

DOI: 10.1002/fam

Table V. *Continued*.

Connection	Failure mode	Equation
j	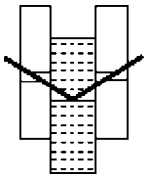	$F_{v,Rk} = 1.25\left\{1.05\frac{f_{h,1,k}t_1 d}{2+\beta}\left[\sqrt{2\beta(1+\beta)+\frac{4\beta(2+\beta)M_{y,Rk}}{f_{h,1,k}\mathrm{d}t_1^2}}-\beta\right]\right\}$
k	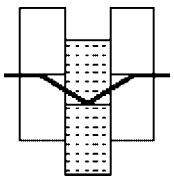	$F_{v,Rk} = 1.25\left\{1.15\sqrt{\frac{2\beta}{1+\beta}}\sqrt{2M_{y,Rk}f_{h,1,k}d}\right\}$

Variables	Descriptions	Units
(A)		
t	Timber thickness	mm
f_h	Embedment strength	kN/m^2
$\beta = \frac{f_{h,2,k}}{f_{h,1,k}}$	Characteristic embedment strength ratio	(–)
d	Fastener diameter	mm
M_y	Fastener yield moment design value	kN mm
$F_{v,Rk}$	Resistance per shear plane per fastener	kN
Subscript 1	Side members	(–)
Subscript 2	Centre member	(–)
Subscript k	Characteristic value	(–)

*The description of the variables used in the first half of the table is given in the second half.

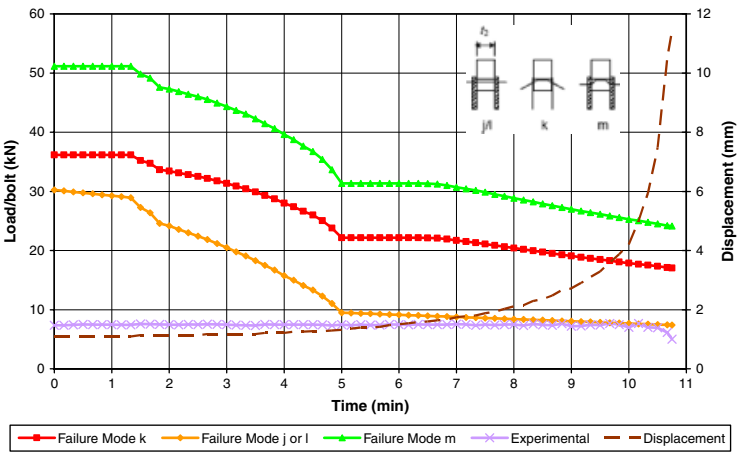

Figure 23. Predicted failure loads for S–W–S bolted connection.

DOI: 10.1002/fam

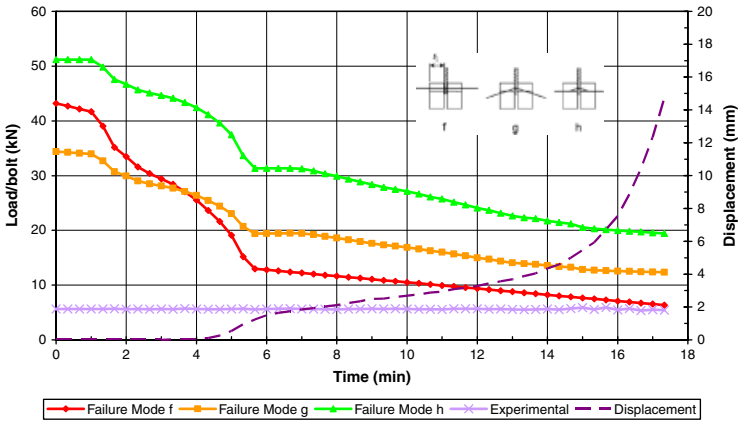

Figure 24. Predicted failure loads for W–S–W bolted connection.

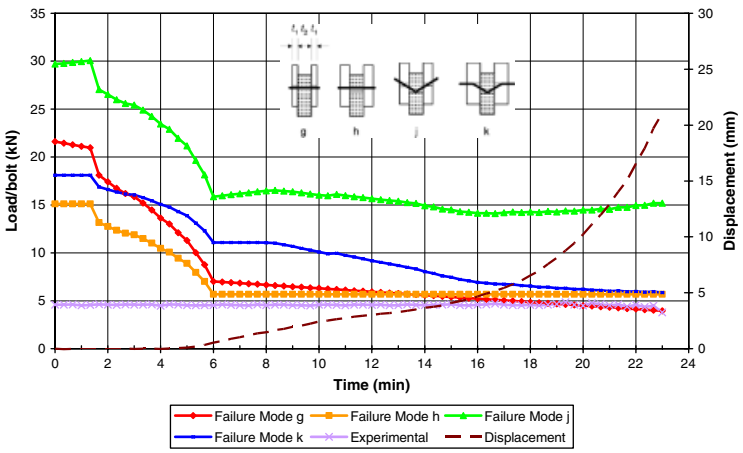

Figure 25. Predicted failure loads for W–W–W bolted connection.

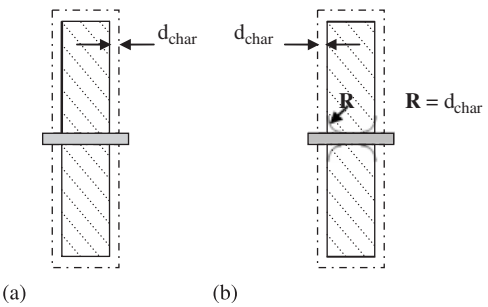

Figure 26. Schematic drawings of (a) the standard model and (b) the modified model.

DOI: 10.1002/fam

Figures 23–25 also show the total joint displacement that took place during the fire tests. Failure of the joints was due to the rapid increase in displacement that took place.

7. CONCLUSIONS

- Of the three types of connections tested in compression at ambient conditions, the W–W–W and W–S–W connections had similar ultimate strength and the S–W–S connections were found to have lower ultimate strength.
- In the ambient tests, failure was caused by longitudinal splitting in the LVL at the bolt positions. A greater end distance could be used to increase the failure load.
- During furnace testing, the connections with mostly wood exposed to the fire (W–W–W and W–S–W) lasted much longer than those with large areas of exposed steel (S–W–S) where there was higher heat transfer into the connection via the steel side plates.
- The failure times in the non-standard furnace testing were converted to standard fire resistance times by two methods, which gave similar results. One method was based on comparing measured char depths and the other was based on the total radiant heat exposure concept.
- The embedment strength of LVL can be described by a bi-linear relationship that varies linearly from $0.04\,kN/mm^2$ at 20°C to $0.015\,kN/mm^2$ at 115°C, and remains constant for temperatures above 115°C.
- This bi-linear embedment strength was used in conjunction with Johansen's yield equations to predict the failure load and the results showed reasonable agreement with the experimental values.
- Since these tests were carried out using a small-scale furnace, it would be prudent to confirm the results using tests carried out in larger furnaces.
- Owing to the high thermal conductivity of steel, there was very little difference in temperature at different locations along the bolts when the connection is exposed to high temperatures. The average timber member temperatures were generally lower than the bolt temperatures due to the poor heat conduction of wood. The exception is the S–W–S connection where the timber and bolt temperatures are comparable.

ACKNOWLEDGEMENTS

Thanks to Carter Holt Harvey for financial support of this programme and supply of all the LVL, which was tested, under the guidance of Hank Bier and Ross Davison. Thanks also to Bob Wilsea-Smith and Grant Dunlop for laboratory support.

REFERENCES

1. Young SA, Clancy P. Compression mechanical properties of wood at temperatures simulating fire conditions. *Fire and Materials* 2001; **25**:83–93.
2. Reszka P, Torero JL. In depth temperature measurements of timber in fires. *The 4th International Workshop on Structures in Fire*, Aveiro, Portugal, 2006.
3. Jong F, Clancy P. Compression properties of wood as functions of moisture, stress, and temperature. *Proceedings of the 2nd International Workshop on Structures in Fire*, Christchurch, New Zealand, 2002; 223–242.
4. Janssens M. Modeling of the thermal degradation of structural wood members exposed to fire. *Proceedings of the 2nd International Workshop on Structures in Fire*, Christchurch, New Zealand, 2002; 211–222.

DOI: 10.1002/fam

5. Frangi A, Mischler A. Fire tests on timber connections with dowel type fasteners. *Working Commission W18—Timber Structures*, *Meeting 37*, International Council for Research and Innovation in Building and Construction, Edinburgh, U.K., August 2004.
6. Erchinger C, Frangi A, Mischler A. Fire behaviour of multiple shear steel-to-timber connections with dowels. *Working Commission W18—Timber Structure*, *Meeting 38*, International Council for Research and Innovation in Building and Construction, Karlsruhe, Germany, 2005.
7. Erchinger C, Frangi A, Mischler A. Thermal investigations on multiple shear steel-to-timber connections. *Proceedings of the World Conference on Timber Engineering*, Portland, OR, U.S.A., 2006.
8. Laplanche K, Dhima D, Racher P. Thermo-mechanical modelling of the timber connection under fire using 3D finite element model. *Proceedings of the World Conference on Timber Engineering*, Portland, OR, U.S.A., 2006.
9. Schabl S, Turk G. Coupled heat and moisture transfer in timber beams exposed to fire. *Proceedings of the World Conference on Timber Engineering*, Portland, OR, U.S.A., 2006.
10. Moraes PD, Rogaume Y, Bocquet JF, Triboulot P. Influence of temperature on the embedding strength. *Holz als Roh- und Werkstoff* 2005; **63**:297–302.
11. Chapuis S, Moraes PD, Rogaume Y, Torero JL. Evaluation of in-depth temperature distributions and embedding resistance of timber in a fire, Private communication, 2006.
12. Chuo TCB. Fire performance of connections in LVL structures. *Fire Engineering Research Report 07/4*, Department of Civil Engineering, University of Canterbury, New Zealand. http://www.civil.canterbury.ac.nz/fire/fe_resrch_reps.shtml, 2007.
13. EC5 2004. *Eurocode 5*: *Design of Timber Structures. EN 1995-1-1:2004*: *Common Rules and Rules for Buildings*. European Committee for Standardization: Brussels, Belgium.
14. Lau PH. Fire resistance of connections in laminated veneer lumber. *Fire Engineering Research Report 06/3*, Department of Civil Engineering, University of Canterbury, New Zealand. http://www.civil.canterbury.ac.nz/fire/fe_resrch_reps.shtml, 2006.
15. Futurebuild. *Span Tables for Residential Building*. Carter Holt Harvey, Auckland, New Zealand, 2002.
16. SNZ 1993. *Code of Practice for Timber Design. NZS 3603*: *1993*. Standards New Zealand: Wellington, New Zealand, 1993.
17. ISO 834. *Fire Resistance Testing*. International Standards Organization: Geneva, 2000.
18. Harris S. Fire resistance of epoxy-grouted steel rod connections in laminated veneer lumber (LVL). *Fire Engineering Research Report 04/7*, Department of Civil Engineering, University of Canterbury, New Zealand, 2004.
19. Buchanan AH. *Structural Design for Fire Safety*. Wiley: Chichester, U.K., 2001.
20. Lane W, Buchanan AH, Moss PJ. Fire performance of laminated veneer lumber (LVL). *Proceedings of the 18th Australasian Conference on the Mechanics of Structures and Materials*. Balkema: Perth, Australia, 2004.
21. Nyman JF. Equivalent fire resistance ratings of construction elements exposed to realistic fires. *Fire Engineering Research Report 02/13*, University of Canterbury, New Zealand, 2001.
22. König J. Structural fire design according to Eurocode 5—design rules and their background. *Fire and Materials* 2005; **29**:147–163.
23. ISO 10984-2. *Timber Structures—Dowel-type Fasteners—Part 2*: *Determination of Embedding Strength and Foundation Values*. International Standards Organization: Geneva, 1999.

DOI: 10.1002/fam